

Two-neutron capture reactions and the r process

Amy Bartlett, Joachim Görres, Grant J. Mathews, Kaori Otsuki, and Michael Wiescher
Department of Physics, University of Notre Dame, Notre Dame, Indiana 46556, USA

Dieter Frekers
Institut für Kernphysik, Westfälische Wilhelms Universität Münster, D-48149 Münster, Germany

Alberto Mengoni
CERN, CH-1211 Geneva 23, Switzerland

Jeffrey Tostevin
Department of Physics, School of Electronics and Physical Sciences, University of Surrey, Guildford, Surrey GU2 7XH, United Kingdom
 (Received 22 February 2005; revised manuscript received 30 March 2006; published 12 July 2006)

Rates for the ${}^4\text{He}(2n, \gamma){}^6\text{He}$ and ${}^6\text{He}(\alpha, n){}^9\text{Be}$ reactions have been calculated, including both resonant and nonresonant contributions. The sequential two-neutron capture process on ${}^4\text{He}$ has also been reevaluated on the basis of new experimental results. It is shown that a one-step dineutron capture reaction may enhance the sequential two-neutron reaction rate by several orders of magnitude. This opens the possibility that reaction flow through ${}^4\text{He}({}^2n, \gamma){}^6\text{He}(\alpha, n){}^9\text{Be}$ may occur in competition with the bottle-neck three-body reactions ${}^4\text{He}(2\alpha, \gamma){}^{12}\text{C}$ and the ${}^4\text{He}(\alpha n, \gamma){}^9\text{Be}$ that initiate the α process and provide seed nuclei for the r process. Here we explore the effect of such dineutron capture on r -process nucleosynthesis. We show that such reactions have little effect on the final abundance and would change only r -process abundances in an extremely neutron-rich low-temperature r process.

DOI: [10.1103/PhysRevC.74.015802](https://doi.org/10.1103/PhysRevC.74.015802)

PACS number(s): 21.45.+v, 21.10.Gv, 24.10.-i, 26.30.+k

I. INTRODUCTION

The rapid neutron capture process, or r process, is one of the dominant mechanisms for producing heavy nuclei with masses above $A = 60$. The r process is characterized by a series of rapid neutron-capture reactions, photodisintegration processes, and β decays that convert initial seed nuclei into heavier neutron-rich elements [1,2]. A reliable prediction of r -process nucleosynthesis requires not only knowledge of these reaction rates but also accurate modeling of the production of seed abundances and the neutron flux. The present work is concerned with clarifying the production mechanism for nuclear seed material.

The actual astrophysical site of the r process is still under debate [3–5], but among the currently favored sites is the high-entropy neutrino-heated environment above the nascent protoneutron star [6–10] in a core-collapse supernova or the shock ejection of neutronized low-entropy material via supernovae [11] or merging neutron stars [4]. In the high-entropy neutrino-energized bubble, the seed abundance is assembled in statistical equilibrium from free protons, neutrons, and α particles via the α process [6,12–14] as material is ablated by neutrino heating within seconds after the core bounce. The α process is limited, however, by the rate of reactions to bridge the unstable mass gaps at $A = 5$ and 8, i.e., the (3α) and $(\alpha + \alpha + n)$ three-particle fusion processes that produce ${}^{12}\text{C}$ and ${}^9\text{Be}$, respectively.

Of particular importance for the present paper, however, is an alternative reaction path through the $A = 5, 8$ gap via a series of dineutron capture processes on ${}^4\text{He}$ and ${}^6\text{He}$. It has been suggested [4–12,15–18] that these reactions might

contribute in neutron-rich r -process environments. Recent r -process simulations, however, have suggested [12] that the rates for this reaction link are insufficient to produce a substantial change in the reaction flow toward heavier elements in high-entropy environments. The possibility remains, however, for this process to contribute in low-entropy, neutron-rich environments. In the present work we therefore extend the earlier studies by considering neutron-rich r -process environments with much lower entropy. We examine the question as to whether the reaction ${}^6\text{He}(\alpha, n){}^9\text{Be}$, combined with a significantly enhanced ${}^4\text{He}(2n, \gamma){}^6\text{He}$ rate could indeed bridge these gaps and significantly affect the subsequent r -process nucleosynthesis.

One purpose of this article, therefore, is to determine the reaction rates for these two reactions. Indeed, we show that the reaction rate for the ${}^4\text{He}(2n, \gamma){}^6\text{He}$ increases when new experimental data about the level structure of the ${}^6\text{He}$ halo nucleus is taken into account. Moreover, there is a second mechanism that has been neglected in previous estimates that concentrated entirely on a sequential neutron capture mechanism [19,20]. Specifically, in this article we investigate the possibility of the dineutron capture process ${}^4\text{He}({}^2n, \gamma){}^6\text{He}$. This requires an analysis of both the possibility of formation and the subsequent capture of a dineutron at the high-density conditions appropriate to the r process. This capture is dominated by a nonresonant direct capture mechanism that has been calculated in the framework of a potential model [21].

In the following sections we describe the derivation of the ${}^4\text{He}({}^2n, \gamma){}^6\text{He}$ reaction rate. We also attempt a first

estimate of the rate of the subsequent ${}^6\text{He}(\alpha, n){}^9\text{Be}$ process independently through a one-level resonance model, taking into account possible interference effects between the broad resonance states in the compound nucleus ${}^{10}\text{Be}$ [23]. In the last section we compare the reaction rate for two-neutron capture with rates of the competing triple- α and α - α - n reaction as links to the higher mass range. We then illustrate the development of the α -process and r -process nucleosynthesis in the framework of various schematic parametrized r -process simulations [22].

II. TWO-NEUTRON CAPTURE REACTIONS ON ${}^4\text{He}$

Three particle reactions in high-density, high-temperature stellar environments typically occur through a two step mechanism. The first step is the formation of an intermediate particle-unbound component, which is in equilibrium between formation through scattering and decay. The second step is the subsequent capture of a second particle on the equilibrium abundance. This approach has been the basis of formulating the triple- α reaction rate through the α unbound ${}^8\text{Be}$ nucleus [24] as well as for the $\alpha + \alpha + n$ reaction through the equilibrium abundance of ${}^8\text{Be}$ [19] with subsequent neutron capture or, additionally, through ${}^5\text{He}$ [25] with subsequent α capture. A third three-particle fusion process, the ${}^4\text{He}(2n, \gamma){}^6\text{He}$ reaction, may take place in environments with a large neutron abundance.

In previous work the ${}^4\text{He}(2n, \gamma){}^6\text{He}$ reaction rate was calculated in a sequential neutron-capture formalism, taking into account only the abundance distribution of neutron-unbound ${}^5\text{He}$ as an intermediate state [19,20]. It was shown that the reaction rate for the sequential two-neutron capture process is determined by the contribution of the broad 2^+ d -wave resonance state at 1.78 MeV in ${}^6\text{He}$ and the p -wave direct neutron capture to the ground state in ${}^6\text{He}$. The reaction rate for this process is determined by the neutron separation energy of ${}^5\text{He}$. Because ${}^5\text{He}$ is unbound by 0.8 MeV the equilibrium abundance for ${}^5\text{He}$ is prohibitively small. The resonant neutron-capture rate on ${}^5\text{He}$ is determined by the $E2 \gamma$ -decay width of the 1.78-MeV state in ${}^6\text{He}$. In Ref. [19] a value of $B(E2, 2^+ \rightarrow 0^+) = 0.57 e^2 \text{fm}^4$ was used. This implies a γ width of $8.8 \mu\text{eV}$ for decay from the excited state at 1.78 MeV to the ground state in ${}^6\text{He}$. More recently, however, a study of the three-body breakup of ${}^6\text{He}$ gave a value of $B(E2, 0^+ \rightarrow 2^+) = (3.2 \pm 0.6) e^2 \text{fm}^4$ [26]. This implies a $B(E2, 2^+ \rightarrow 0^+)$ value of $0.64 e^2 \text{fm}^4$ and a γ width of $9.88 \mu\text{eV}$. Although this result suggests a small increase in the resonant component, the value for the dominating direct capture to the ground state still depends on the single-particle structure of the ${}^6\text{He}$ ground state.

Because the ground-state structure of ${}^6\text{He}$ is characterized by a two-neutron skin, we have calculated the possibility of its formation through dineutron (2n) capture on ${}^4\text{He}$. The dineutron capture rate has been estimated using a similar formalism as used for deriving the two neutron sequential capture rate [19]. Both successive neutron capture and dineutron capture are two-step reactions. Consequently, the reaction rate $\langle 1nn \rangle$ for both these three-particle reactions is described

by a double integral,

$$N_A^2 \langle 1nn \rangle = N_A^2 \int_{E_1} \frac{d\langle (n, n) \rangle(E_1)}{dE_1} \frac{2\hbar}{\Gamma(E_1)} \times \left[\int_{E_2} \frac{d\langle (n, \gamma) \rangle(E_1, E_2)}{dE_2} dE_2 \right] dE_1, \quad (1)$$

where the integrands are given by

$$\frac{d\langle \sigma v \rangle}{dE} = \sqrt{\frac{8}{\pi \mu}} \frac{1}{(kT)^{3/2}} \sigma(E) \exp\left(-\frac{E}{kT}\right). \quad (2)$$

The term $\langle n, n \rangle$ refers to the rate for the first reaction step of ${}^4\text{He} + n$ or $n + n$ scattering at a collision energy of E_1 . The term $\langle n, \gamma \rangle$ refers to the second step, i.e., the capture rate of the second neutron on ${}^5\text{He}$ or the rate for the dineutron capture on ${}^4\text{He}$ with E_2 as the collision energy. The $\Gamma_2(E_1)$ is the energy-dependent width of the intermediate nucleus, which in the first case is the ground state of ${}^5\text{He}$, and in the case of dineutron capture, is the width of the virtual dineutron state.

The cross section for elastic neutron scattering $\sigma_{n,n}(E)$ has been directly derived from the neutron-neutron scattering length $a_{nn} = -18.6 \pm 0.4$ fm, as recently confirmed through the (${}^2\text{H}, {}^2\text{He}$) charge-exchange experiment [27]. Figure 1 shows the resultant n - n -scattering cross-section. Because the energy of the ${}^1S_0 nn$ virtual state is very close to zero energy the physical nn cross section increases as $E_1 \rightarrow 0$. Here, we have approximated the dineutron state as a 0^+ resonance with a width of $\Gamma_2(E_1) = 0.095$ MeV derived from fitting the scattering cross-section curve.

The second reaction (dineutron capture on ${}^4\text{He}$) has a Q value of 0.973 MeV. The cross section is determined by resonant capture and direct capture contributions. The resonant term is dominated by a d -wave dineutron capture into the 1.797 MeV $J^\pi = 2^+$ state with a resonance energy of $E_r = 0.824$ MeV. This state decays by $E2 \gamma$ emission to the ground state. In direct capture the dineutron is captured into the ground state of ${}^6\text{He}$. The strength of the resonance is rather weak,

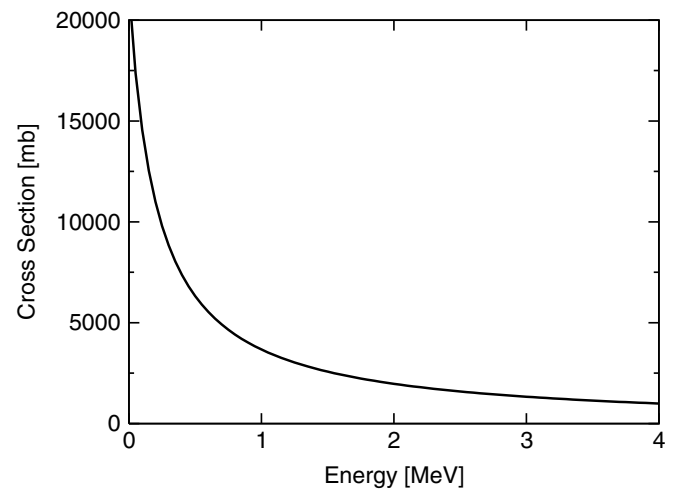


FIG. 1. The n - n -scattering cross section as calculated from the neutron-neutron scattering length $a_{nn} = -18.6$ fm for a radius of $r = 2.8$ fm [27].

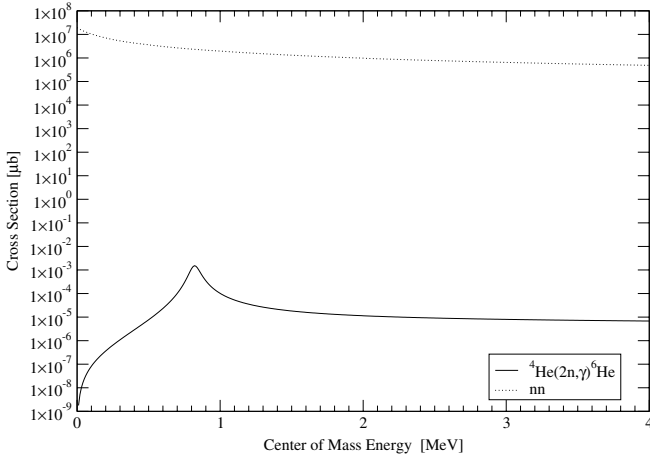


FIG. 2. Cross section for the dineutron capture reaction on ${}^4\text{He}$ compared to the n - n -scattering cross section.

$\omega\gamma \approx 50 \mu\text{eV}$, as estimated from the experimental γ partial width of $\Gamma(E2) = 9.88 \mu\text{eV}$. For calculating the direct capture, a s -wave configuration for the ${}^6\text{He}$ ground state was adopted in terms of a simple two-cluster model ${}^4\text{He} \otimes {}^2n$. With this configuration the direct capture is dominated by an $E1$ $p \rightarrow s$ transition. The cross section has been calculated in terms of a potential model [21] assuming a dineutron spectroscopic factor of $C^2S_{2n} = 0.5$. The result of this model calculation is consistent with the results of the ${}^6\text{He} \rightarrow {}^4\text{He} + 2n$ Coulomb dissociation data [26]. The resulting capture cross section for both resonant d -wave and nonresonant p -wave capture is shown in Fig. 2. These are compared with the cross section of the previously estimated sequential two-neutron capture process.

Figure 3 shows the reaction rate for both the sequential two-neutron and dineutron capture on ${}^4\text{He}$ as a function of temperature. This figure demonstrates that the second process dominates by more than five orders of magnitude. This is mainly because of the large difference in the neutron

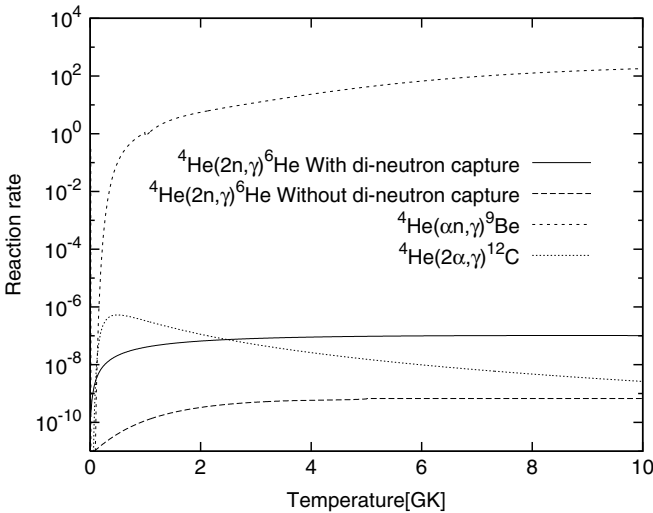


FIG. 3. Reaction rate for the dineutron capture ${}^4\text{He}(2n, \gamma){}^6\text{He}$ reaction compared with the previously determined reaction rate for a sequential two-neutron capture ${}^4\text{He}(2n, \gamma){}^6\text{He}$ mechanism.

separation energy of the two possible intermediate nuclei ${}^5\text{He}$ ($S_n = -0.8 \text{ MeV}$) and 2n ($S_n = 0 \text{ MeV}$). Also shown are the reaction rates for the two competing three-particle reactions ${}^4\text{He}(2\alpha, \gamma){}^{12}\text{C}$ and ${}^4\text{He}(\alpha n, \gamma){}^{12}\text{C}$ as a function of temperature. This figure clearly demonstrates that, in all three cases, the reaction rates are of similar strength at temperatures $T \geq 10^8 \text{ K}$.

III. ${}^6\text{He}(\alpha, n){}^9\text{Be}$ REACTION RATE

The reaction rate for ${}^6\text{He}(\alpha, n){}^9\text{Be}$ is determined by several broad overlapping resonances. The α unbound levels in the compound nucleus ${}^{10}\text{Be}$ above the α threshold ($S_\alpha = 7.412 \text{ MeV}$) are well known [28,29]. The low-energy-reaction cross section is dominated by a 2^+ resonance state at $E_x = 7.542 \text{ MeV}$ and by the low-energy tails of several higher-energy resonance states above 9.3 MeV . The level parameters are reasonably well known [29] or have been determined from the available experimental data on ${}^{10}\text{Be}$. The 2^+ state at 7.542 MeV has a width of $6.3 \pm 0.8 \text{ keV}$ and has recently been identified [30] as a highly deformed α - α - $2n$ chain configuration with an unusually large α partial width of $\Gamma_\alpha = 22 \pm 8 \text{ eV}$. The ratio of $\Gamma_\alpha / \Gamma = 0.0035 \pm 0.0012$ yields a neutron partial width of $\Gamma_n = 6280 \text{ eV}$. The 2^+ excited state at 9.560 MeV has a total width of $\Gamma = 141 \pm 10 \text{ keV}$. The partial widths are derived from the ratio $\Gamma_\alpha / \Gamma = 0.16 \pm 0.04$. The excited state at 10.150 MeV has been identified as a 3^- member of the $K^\pi = 1^-$ band in ${}^{10}\text{Be}$ [30,31]. The total width has been determined to be $\Gamma_{\text{tot}} = 296 \pm 16 \text{ keV}$. Earlier measurements indicated a small neutron partial width [32]; we have therefore adopted $\Gamma_n \approx 10 \text{ keV}$. The level at 10.57 MeV has been suggested [30] as the 4^+ member of the $K^\pi = 0^+$ rotational band. Because no information is available about the width of the state ($\Gamma_{\text{tot}} \leq 150 \text{ keV}$, we calculated the partial widths using a WKB approximation by adopting the single-particle and the α -cluster configuration of the state from the 2^+ member of the band at 7.5 MeV (see discussion above) [30].) The level at $E_x = 11.76 \text{ MeV}$ excitation energy has a total width of $\Gamma_{\text{tot}} = 121 \pm 10 \text{ keV}$. No spin assignment has been made. We adopted a spin of $J^\pi = 0^+$ on the basis of a theoretical analysis of molecular orbital structure in ${}^{10}\text{Be}$ [33] that predicted a $J^\pi = 0^+$ member of the $K^\pi = 0^+$ ground-state band at 11.6 MeV excitation energy. The partial widths were determined from a ratio of $\Gamma_\alpha / \Gamma_n = 0.1$ adopted from the other band member states. All resonance level parameters are summarized in Table I.

On the basis of these parameters the total cross section has been estimated in terms of a single-level Breit-Wigner formalism, including possible interference effects between the 2^+ resonance states. Figure 4 shows the calculated cross section for the ${}^6\text{He}(\alpha, n){}^9\text{Be}$ reaction up to 5 MeV of α energy. The reaction rate was calculated by averaging over the usual Maxwellian distribution for temperature T ,

$$\langle \sigma v \rangle = \sqrt{\frac{8}{\pi \mu}} \frac{1}{(kT)^{\frac{3}{2}}} \int_0^\infty \sigma(E) E \exp\left(-\frac{E}{kT}\right) dE, \quad (3)$$

where μ is the reduced mass.

TABLE I. Resonance level parameters in the compound nucleus ^{10}Be for the $^6\text{He}(\alpha, n)^9\text{Be}$ reaction rate.

| E_R/MeV | J^π | $\Gamma_{\text{tot}}(E_R)$ | Spectroscopic factors | | Widths | | Resonant cross-section $\sigma(E_R)$ |
|------------------|---------|----------------------------|-----------------------|-----------------------|-----------------------|------------------------|---|
| | | | C^2S_α | C^2S_n | $\Gamma_\alpha(E_R)$ | $\Gamma_n(E_R)$ | |
| 7.542 | 2^+ | 6.3×10^{-3} | 0.1 | 3.05×10^{-3} | 8.64×10^{-8} | 6.299×10^{-3} | $16.58 \mu\text{b}$ |
| 9.64 | 2^+ | 0.291 | 2.23×10^{-2} | 3.21×10^{-2} | 0.034 | 0.26 | 96.8 mb |
| 10.15 | 3^- | 0.310 | 0.40 | 8.51×10^{-3} | 0.281 | 0.028 | 0.104 b |
| 10.57 | 4^+ | 0.150 | 5.03×10^{-2} | 0.23 | 0.01 | 0.14 | 96.7 mb |
| 11.76 | 4^+ | 0.121 | 0.15 | 1.3×10^{-2} | 0.104 | 0.017 | 0.170 b |

No significant differences ($\leq 4\%$) were observed between the rates calculated for constructive and destructive interference. Figure 5 shows the reaction rate of $^6\text{He}(\alpha, n)^9\text{Be}$ as a function of temperature.

IV. IMPACT ON NEUTRON FLUX AND r -PROCESS NUCLEOSYNTHESIS

Despite decades of study, the astrophysical site for the main r -process component is still unknown. There are three dominant candidates: neutrino-driven winds in Type II supernovae; the prompt explosion of low-mass supernovae; and neutron star mergers. The conditions for the r -process nucleosynthesis, such as the temperature and density profile, are significantly different in each of these candidate environments. Although there have been many theoretical nucleosynthesis studies aimed at testing the viability of those models none of them has reached a definitive conclusion. This uncertainty is in part because of to the difficulty of modeling of such explosive events. We have assumed simple schematic parametrizations for each of the environments as described below.

Our nucleosynthesis code is based on the dynamical network described in Meyer *et al.* [7], which has been extended by Terasawa and Orito [22,34]. This code calculates dynamically the r process and its seed production simultaneously. We terminated our calculation when the neutron abundance

Y_n became less than 10^{-15} , by which point the abundance distribution is no longer affected by neutron capture. We adopted a primitive fission recycling model, which assumes that all elements with $A = 260$ immediately break into two symmetric nuclei. For each of the models considered, we have calculated the nucleosynthesis yields with three networks: (i) without any reactions to form ^6He , (ii) with the $^4\text{He}(2n, \gamma)^6\text{He}$ included, and (iii) with both the $^4\text{He}(2n, \gamma)^6\text{He}$ and $^4\text{He}(^2n, \gamma)^6\text{He}$ reactions included.

A. Neutrino-driven winds

The proton-neutron stars born in Type II supernovae release their energy via neutrinos during their Kelvin-Helmholtz cooling phase. Those neutrinos heat up material on the surface and eject them into a high-entropy bubble above the neutron star. This is the so-called neutrino-driven wind (e.g., Refs. [15,36]). Because the energy of antineutrinos is higher than electron neutrinos, the wind material becomes slightly neutron-rich. If the entropy is high enough, it becomes a suitable environment for the main r process. Although this is a popular model, there are several problems in this model. For example, it is still controversial as to whether such high entropy is actually realized in the wind (e.g., Ref. [36] and reference therein). In addition, Meyer *et al.* [14] pointed out that neutrino

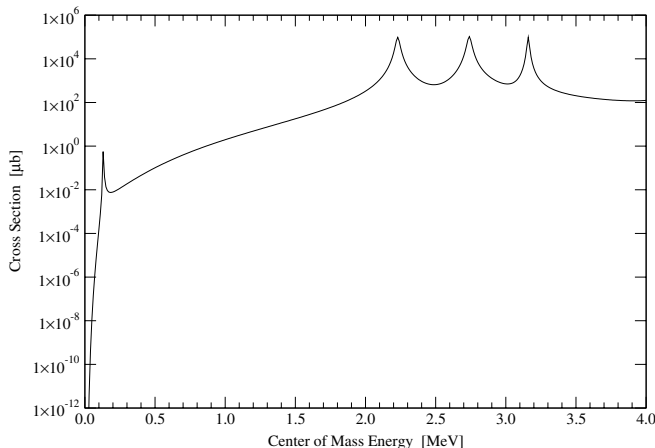


FIG. 4. Calculated cross section for the $^6\text{He}(\alpha, n)^9\text{Be}$ reaction as a function of energy.

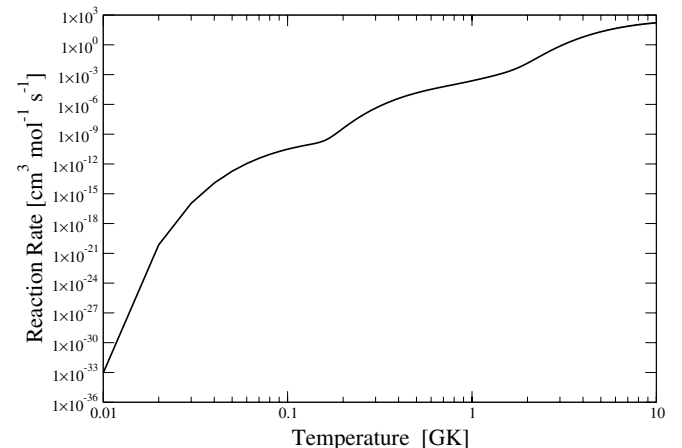


FIG. 5. Reaction rate for the $^6\text{He}(\alpha, n)^9\text{Be}$ reaction as a function of temperature.

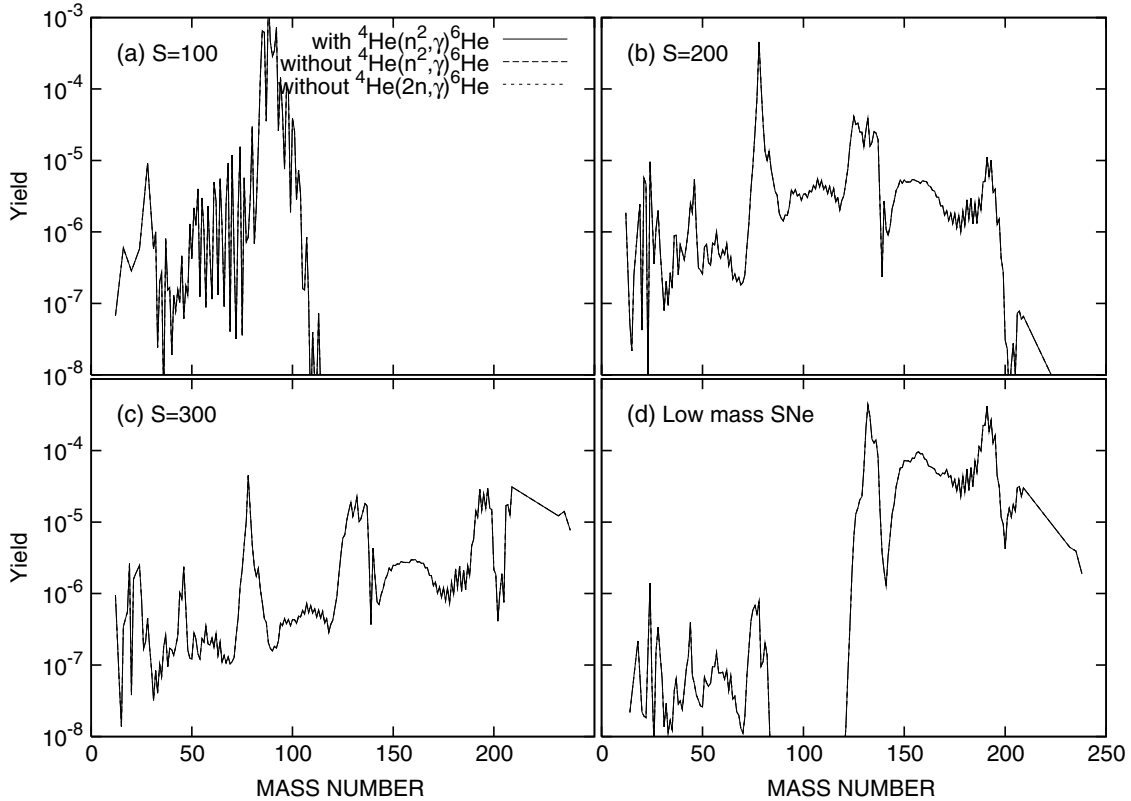


FIG. 6. Final r -process abundance distributions in neutrino-driven wind models (a)–(c) and the low-mass supernovae model (d). Lines are drawn for models with (solid lines) and without (dashed line) dineutron capture, and without any ${}^6\text{He}$ reaction flow (dotted line) for various values of entropy per baryon as labeled. There is essentially no effect from the flow through ${}^6\text{He}$ in these models.

interactions with nuclei during the r process increases the electron fraction. Higher entropy and/or a shorter time scale may thus be necessary to realize suitable conditions for the r process in this model when neutrino effects are considered.

We assume an exponential adiabatic expansion model for the neutrino-driven wind. This model is often invoked in parametric studies of high-entropy environments (Ref. [35]). In this model, the density and temperature profiles are given as

$$T_9 = 9.0 \exp(-t/t_{\text{exp}}) + 0.6 \quad (4)$$

$$\rho = 3.3 \times 10^5 T_9^3 / S, \quad (5)$$

where T_9 is the temperature in units of 10^9 , t_{exp} is the expansion time scale, ρ is the baryon matter density in g/cm^{-3} , and S is the entropy per baryon. We chose a parameter set of $t_{\text{exp}} = 0.05$ sec and $Y_e = 0.45$ and calculated different entropies of $S = 100, 200, 300$.

Figures 6(a)–6(c) show the final abundance distribution for the neutrino-driven wind model cases. There is essentially no difference between these cases with three different network calculations. The reason is simply that for higher-entropy environments the small binding energy of ${}^6\text{He}$ means that the photodisintegration of ${}^6\text{He}$ is rapid and prohibits substantial reaction flow through ${}^6\text{He}$. From this analysis we conclude that dineutron capture should have little influence on neutrino-

energized wind models for r -process nucleosynthesis, justifying the neglect of this effect in earlier studies.

B. Low-mass supernovae

Low-mass core-collapse SNe ($8\text{--}12 M_{\odot}$) are another candidate. If such low-mass supernovae explode, they would occur via a prompt explosion. During such prompt explosions, relatively low entropy ($\sim 15k$), and a low electron fraction ($Y_e \sim 0.2$), can be realized (e.g., Refs. [11,16,17]). These are also ideal conditions for the r process. The main objection to this model is the explosion mechanism itself. It is still unclear as to whether such light supernovae actually explode. This is exacerbated by the fact that there is no convincing observational evidence of the remnants of such explosions.

For these calculations, we have assumed that the material expands exponentially, $\rho \propto \exp(-t/t_{\text{exp}})$. Here, t_{exp} is the expansion time scale. Corresponding temperatures are obtained from the equation of state of Timmes and Swesty [18]. As used in previous studies, we adopted the entropy to be $S = 15$ and $Y_e = 0.2$.

Figure 6(d) shows a result for the low-mass supernovae model. There is no significant difference between the three network calculations. We calculated the case with $t_{\text{exp}} = 0.05$ sec for $T_9 > 1.0$ and $t_{\text{exp}} = 0.3$ sec when the temperature drops below $T_9 < 1.0$ to imitate simulation's results in

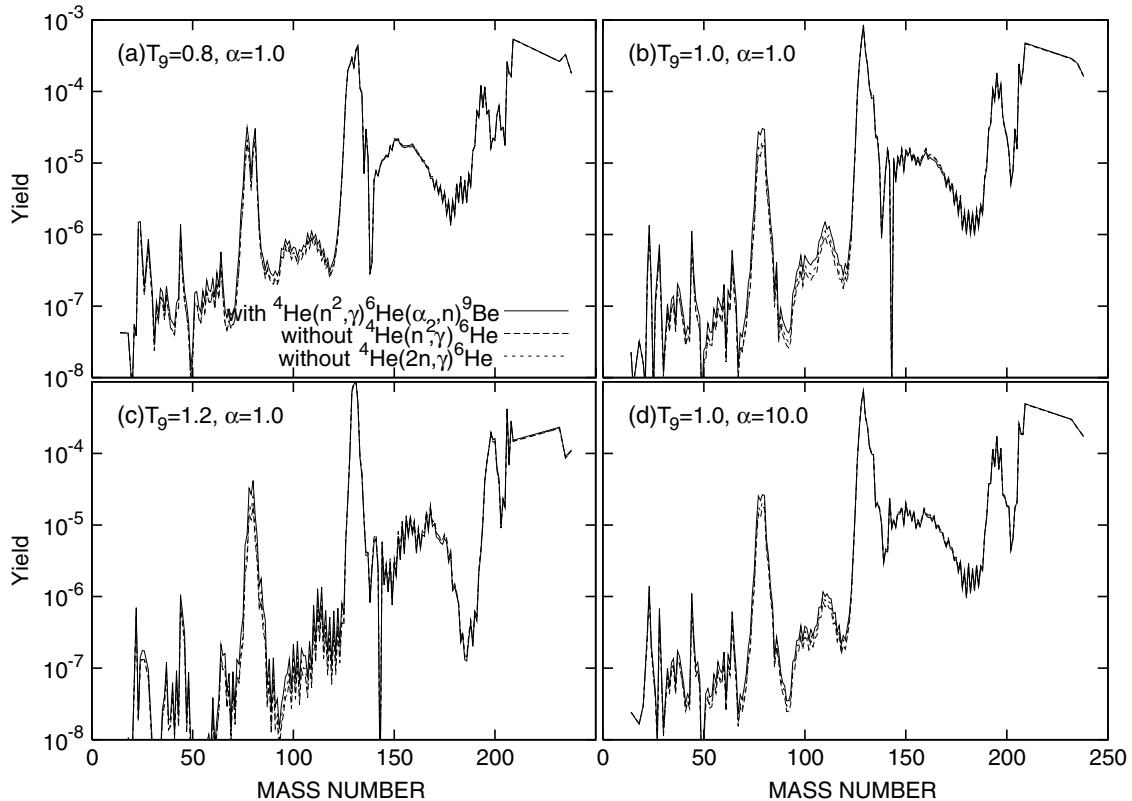


FIG. 7. Final r -process abundance distributions in neutron-star merger models. Models are shown for calculations with (solid lines) and without (dashed line) dineutron capture and without any ${}^6\text{He}$ reaction flow (dotted line). Effects of the capture flow through ${}^6\text{He}$ are most apparent for nuclides with $A < 130$.

previous studies. We also did calculations with different time scales. These, however, did not change the conclusions discussed here.

C. Neutron star mergers

Another neutron-rich environment could be realized in neutron star mergers (e.g., Ref. [4]). In this model the entropy is very low, but the electron fraction is also very low. It is the most neutron-rich environment among the three models considered here. Although theoretical calculations show reasonable yields, this model encounters some difficulties in explaining the chemical enrichment history of the galaxy [10].

For the other two models, the heating from nucleosynthesis can be shown to be negligible. However, in the neutron star merger model, heating from β decays and fission can significantly affect the temperature profiles. Because the current version of our network code does not take heating from nucleosynthesis into account, we have assumed a constant temperature $T_9 = 0.8, 1.0, 1.2$. In other r -process calculations in the neutron star merger model, the temperature varies between 0.2 to 1.2×10^9 K during the r process [4]. Hence, a constant temperature is a reasonable assumption for our purposes of testing the impact of new nuclear reaction flows. Initial conditions for this model are from Tables 1 and 2 in, Ref. [13]. Here, we assume that the material expands on a free fall time scale ($\alpha = 1.0$) and the electron fraction is initially set to $Y_e = 0.15$ and an initial proton abundances

$Y_p = 1.0 \times 10^{-4}$. We also calculated a model with a faster expansion time scale ($\alpha = 10$) with a constant temperature $T_9 = 1.0$, and $Y_e = 0.15$.

Figure 7 shows the abundance distribution in the low-entropy r process with three different network calculations. Here we see that dineutron capture can make some difference in the light nuclei with $A < 130$, but it is not significant for heavier elements. Figure 8 shows the specific effects on the abundances of ${}^{12}\text{C}$ and ${}^{14}\text{C}$ versus time in the case of $T_9 = 1.0, \alpha = 1.0$. Here, we see that there are clear difference between the three different networks in the earlier stage of nucleosynthesis. However, it does not affect the final

TABLE II. Reaction rates for dineutron capture and ${}^6\text{He}(\alpha, n){}^9\text{Be}$.

| T_9 | ${}^4\text{He}(2n, \gamma){}^6\text{He}$ | ${}^6\text{He}(\alpha, n){}^9\text{Be}$ |
|-------|--|---|
| 0.5 | 2.44×10^{-8} | 1.44×10^{-5} |
| 0.8 | 4.06×10^{-8} | 9.99×10^{-5} |
| 1.0 | 5.06×10^{-8} | 2.38×10^{-4} |
| 1.5 | 7.19×10^{-8} | 1.55×10^{-3} |
| 2.0 | 8.88×10^{-8} | 2.81×10^{-2} |
| 2.5 | 1.02×10^{-7} | 2.37×10^{-1} |
| 3.0 | 1.12×10^{-7} | 1.03 |
| 4.0 | 1.28×10^{-7} | 6.32 |
| 5.0 | 1.39×10^{-7} | $1.82 \times 10^{+1}$ |

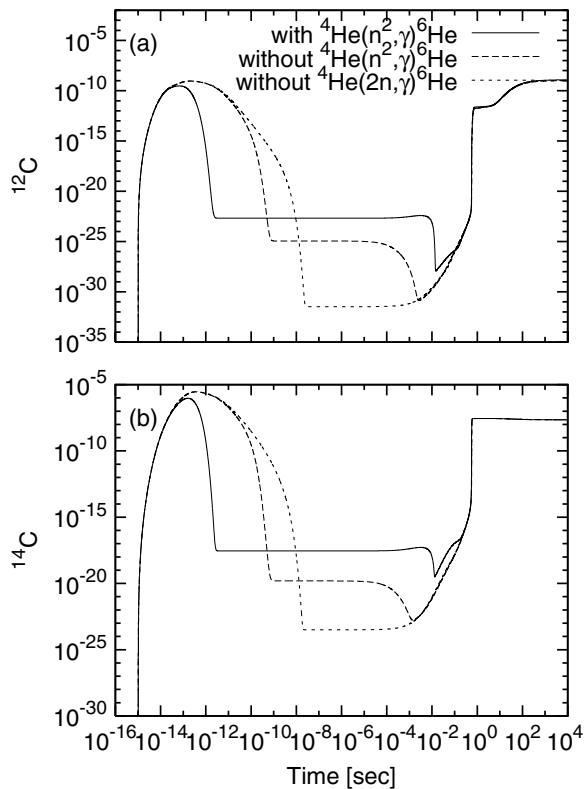


FIG. 8. Abundances of ^{12}C and ^{14}C isotopes versus time in a neutron-star merger model with $T_9 = 1.0$, $\alpha = 1.0$, $Y_e = 1.5$. Effects of the capture flow through ^6He are clearly apparent for earlier stage of nucleosynthesis.

abundances. This is because the environment is so neutron rich that fission recycling obscures the effects of all processes that occurred at an earlier stage of nucleosynthesis.

Fission recycling plays a role in all models, but it is most effective for the neutron-star merger models. Note that there is no significant difference for elements heavier than the second r -process peak in the neutron-star merger model. If we compare snapshots of each calculation, there are large differences at the early stage of nucleosynthesis. But those differences are obscured by fission recycling. This effect of fission recycling could be a hint to explain the apparent robustness of the r process. Because our fission model is very primitive, more realistic, systematic studies of fission recycling are needed for further discussion.

V. SUMMARY AND CONCLUSION

The sequential two-neutron capture process on ^4He has been reevaluated on the basis of new experimental results. We have calculated new reaction rates for the $^4\text{He}(2n, \gamma)^6\text{He}$ and $^6\text{He}(\alpha, n)^9\text{Be}$ reactions in which resonant and nonresonant contributions for both reactions have been taken into account. We have shown that a one-step dineutron capture reaction may enhance the formation of ^6He by several orders of magnitude. This shows that neutron-skin or halo-structure configurations may have an impact on reaction processes with neutron rich nuclei. However, these configurations are not highly bound and are easily depleted by inverse photodisintegration. In the cases discussed here, the photodisintegration of ^6He is so rapid that the effects of dineutron capture are manifest only at very low temperatures and high neutron density. Hence, it is unlikely that a significant reaction flow through $^4\text{He}(^2n, \gamma)^6\text{He}(\alpha, n)^9\text{Be}$ may occur in competition to the $^4\text{He}(2\alpha, \gamma)^{12}\text{C}$ and the $^4\text{He}(\alpha n, \gamma)^9\text{Be}$ three-particle reactions feeding the α process.

We have analyzed the consequences of such dineutron capture in the context of schematic models for r -process nucleosynthesis. We have shown that this new reaction channel is not significant for the high-entropy neutrino-driven wind model or the low-mass supernovae model. It does, however, have a discernible influence on the production of seed material in neutron merger models with very low-entropy low-temperature conditions. Although this new reaction flow does not have a large impact on the final abundances, there are significant differences at the earlier stage of nucleosynthesis. Although our calculation neglected heating from nucleosynthesis and adopted a primitive fission model, we could tentatively conclude that the new reaction flow might impact the final abundances under low-entropy, low-temperature conditions such as may occur in neutron star mergers.

ACKNOWLEDGMENTS

Work at the University of Notre Dame supported by the National Science Foundation through grant PHY02-16783 through the Joint Institute for Nuclear Astrophysics (JINA). One of the authors (G.J.M.) acknowledges support from the U.S. Department of Energy under Nuclear Theory Grant DE-FG02-95-ER40934.

- [1] G. J. Mathews and R. A. Ward, Rep. Prog. Phys. **48**, 1371 (1985).
- [2] B. Pfeiffer, K.-L. Kratz, F.-K. Thielemann, and W. B. Walters, Nucl. Phys. **A693**, 282 (2001).
- [3] G. J. Mathews and J. J. Cowan, Nature **345**, 491 (1990).
- [4] C. Freiburghaus, S. Rosswog, and F.-K. Thielemann, Astrophys. J. **525**, L121 (1999).
- [5] Y.-Z. Qian, Astrophys. J. **534**, L67 (2000).
- [6] S. E. Woosley and R. D. Hoffman, Astrophys. J. **395**, 202 (1992).
- [7] B. S. Meyer, G. J. Mathews, W. M. Howard, S. E. Woosley, and R. D. Hoffman, Astrophys. J. **399**, 656 (1992).
- [8] S. E. Woosley, J. R. Wilson, G. J. Mathews, R. D. Hoffman, and B. S. Meyer, Astrophys. J. **433**, 229 (1994).
- [9] Y.-Z. Qian and G. J. Wasserburg, Astrophys. J. **588**, 1099 (2003).
- [10] D. Argast, M. Samland, F.-K. Thielemann, and Y.-Z. Qian, Astron. Astrophys. **416**, 997 (2004).
- [11] K. Sumiyoshi, M. Terasawa, G. J. Mathews, T. Kajino, S. Yamada, and H. Suzuki, Astrophys. J. **562**, 880 (2001).
- [12] J. Witti, H.-T. Janka, and K. Takahashi, Astron. Astrophys. **286**, 841 (1994).
- [13] B. S. Meyer, Astrophys. J. **343**, 254 (1989).

- [14] B. S. Meyer, T. D. Krishnan, and D. D. Clayton, *Astrophys. J.* **498**, 808 (1998).
- [15] Y.-Z. Qian and S. E. Woosley, *Astrophys. J.* **471**, 331 (1996).
- [16] J. C. Wheeler, J. J. Cowan, and W. Hillebrandt, *Astrophys. J.*, **493**, L101 (1998).
- [17] S. Wanajo, M. Tamamura, N. Itoh, K. Nomoto, Y. Ishimaru, T. C. Beers, and S. Nozawa, *Astrophys. J.* **593**, 968 (2003).
- [18] F. X. Timmes and F. D. Swesty, *Astrophys. J. Suppl.* **126**, 501 (2000).
- [19] J. Görres, H. Herndl, I. J. Thompson, and M. Wiescher, *Phys. Rev. C* **52**, 2231 (1995).
- [20] V. Efros, W. Balogh, H. Herndl, R. Hofinger, and H. Oberhummer, *Z. Phys. A* **355**, 101 (1996).
- [21] A. Mengoni, T. Otsuka, and M. Ishihara, *Phys. Rev. C* **52**, R2334 (1995).
- [22] M. Terasawa, K. Sumiyoshi, T. Kajino, G. J. Mathews, and I. Tanihata, *Astrophys. J.* **562**, 470 (2001).
- [23] D. R. Tilley, C. M. Cheves, J. L. Godwin, G. M. Hale, H. M. Hofmann, J. H. Kelley, and H. R. Weller, *Nucl. Phys. A* **708**, 3 (2002).
- [24] K. Nomoto, F.-K. Thielemann, and S. Miyaji, *Astron. Astrophys.* **149**, 239 (1985).
- [25] L. Buchmann, E. Gete, J. C. Chow, J. D. King, and D. F. Measday, *Phys. Rev. C* **63**, 034303 (2001).
- [26] T. Aumann *et al.*, *Phys. Rev. C* **59**, 1252 (1999).
- [27] C. Bäumer *et al.*, *Phys. Rev. C* **71**, 044003 (2005).
- [28] F. Ajzenberg-Selove, *Nucl. Phys.* **A490**, 1 (1988).
- [29] D. R. Tilley, J. H. Kelley, J. L. Godwin, D. J. Millener, J. Purcell, C. G. Sheu, and H. R. Weller, *Nucl. Phys.* **A745**, 155 (2004).
- [30] J. A. Liendo, N. Curtis, D. D. Caussyn, N. R. Fletcher, and T. Kurtukian-Nieto, *Phys. Rev. C* **65**, 034317 (2001).
- [31] N. Curtis, D. D. Caussyn, N. R. Fletcher, F. Maréchal, N. Fay, and D. Robson, *Phys. Rev. C* **64**, 044604 (2001).
- [32] N. Soić, S. Blagus, M. Bogovac, S. Fazinić, M. Lattuada, M. Milin, D. Miljanić, D. Rendic, C. Spitaleri, T. Tadić, and M. Zadro, *Europhys. Lett.* **34**, 7 (1996).
- [33] N. Itagaki and S. Okabe, *Phys. Rev. C* **61**, 044306 (2001).
- [34] M. Orito, T. Kajino, R. N. Boyd, and G. J. Mathews, *Astrophys. J.* **488**, 515 (1997).
- [35] K. Otsuki, G. J. Mathews, and T. Kajino, *New Astron.* **8**, 767 (2003).
- [36] K. Otsuki, H. Tagoshi, T. Kajino, and S. Wanajo, *Astrophys. J.* **533**, 424 (2000).